Development 136, 2757-2765 (2009) doi:10.1242/dev.034959

The Integrator subunits function in hematopoiesis by modulating Smad/BMP signaling

Shijie Tao[1,2], Yu Cai[1,2] and Karuna Sampath[1,2,3,*]

Hematopoiesis, the dynamic process of blood cell development, is regulated by the activity of the bone morphogenetic protein (BMP) signaling pathway and by many transcription factors. However, the molecules and mechanisms that regulate BMP/Smad signaling in hematopoiesis are largely unknown. Here, we show that the Integrator complex, an evolutionarily conserved group of proteins, functions in zebrafish hematopoiesis by modulating Smad/BMP signaling. The Integrator complex proteins are known to directly interact with RNA polymerase II to mediate 3′ end processing of U1 and U2 snRNAs. We have identified several subunits of the Integrator complex in zebrafish. Antisense morpholino-mediated knockdown of the Integrator subunit 5 (Ints5) in zebrafish embryos affects U1 and U2 snRNA processing, leading to aberrant splicing of *smad1* and *smad5* RNA, and reduced expression of the hematopoietic genes *stem cell leukemia* (*scl*, also known as *tal1*) and *gata1*. Blood smears from *ints5* morphant embryos show arrested red blood cell differentiation, similar to *scl*-deficient embryos. Interestingly, targeting other Integrator subunits also leads to defects in *smad5* RNA splicing and arrested hematopoiesis, suggesting that the Ints proteins function as a complex to regulate the BMP pathway during hematopoiesis. Our work establishes a link between the RNA processing machinery and the downstream effectors of BMP signaling, and reveals a new group of proteins that regulates the switch from primitive hematopoietic stem cell identity and blood cell differentiation by modulating Smad function.

KEY WORDS: Hematopoiesis, Integrator proteins, RNA splicing, Smad/BMP signaling, Zebrafish

INTRODUCTION

Hematopoiesis is the process that gives rise to all types of blood cells. It is generally believed that hematopoietic development branches at an early stage into myeloid and lymphoid cell fates. The lymphoid branch differentiates to T, B and natural killer cells, and the myeloid branch develops into all the other cell types, including monocytes/macrophages, granulocytes, megakaryoctyes and erythrocytes (red blood cells, RBCs) (Hsu et al., 2001; Larsson and Karlsson, 2005). In the mouse, the hemangioblast progenitors (common progenitors for both hematopoietic and endothelial lineages) arise from a mesodermal population of cells positive for brachyury (T) expression (Fehling et al., 2003). Similarly, in zebrafish, hemangioblasts originate from the ventral margin of the embryo (Vogeli et al., 2006). Primitive hematopoiesis occurs at two anatomical sites: the rostral blood island (RBI) arising from the cephalic mesoderm and the intermediate cell mass (ICM) located in the trunk, ventral to the notochord. Cells within the ICM predominantly differentiate into vascular cells and primitive erythrocytes, which enter the blood circulation around 24 hours post fertilization (hpf) (Al-Adhami and Kunz, 1977; Davidson and Zon, 2004).

Recent work has shown that the process of blood cell formation is regulated by a variety of intrinsic transcription factors. These include the Stem cell leukemia (Scl, Tal1 – ZFIN) basic helix-loop-helix transcription factor, and a zinc-finger transcription factor, Gata1. *scl* is expressed in the RBI and the ICM, where its expression marks the formation of primitive hematopoietic stem cells (HSCs) and vascular precursors. *gata1* is expressed in the lateral plate mesoderm that will migrate medially to form the ICM and is crucial for myeloid differentiation (de Jong and Zon, 2005). Many extracellular signaling molecules present in the environment are also involved in hematopoietic regulation. These include the bone morphogenetic proteins (BMPs). BMPs belong to the Transforming growth factor β (TGF-β) family of secreted proteins, and signal via the downstream transcription factors, Smad1, 5 and 8 (Smad9 – ZFIN) (von Bubnoff and Cho, 2001). BMP signaling is important not only for the patterning of ventral mesoderm from where the primitive HSCs arise, but also for regulating the specification and proliferation of blood progenitors (Larsson and Karlsson, 2005; Winnier et al., 1995). Loss of either Smad1 or Smad5 leads to a failure in the generation of definitive hematopoietic progenitors in zebrafish (McReynolds et al., 2007).

Integrator is a multiprotein complex that associates with the C-terminal repeats of RNA polymerase II and mediates U1 and U2 snRNA 3′ end processing (Baillat et al., 2005). Here, we report that the snRNA metabolism-related factor Ints5, a subunit of the Integrator complex, functions in zebrafish hematopoiesis by modulating the splicing of *smad1* and *smad5* RNA, thereby establishing a potential link between the RNA processing machinery and downstream effectors of BMP signaling in the regulation of hematopoiesis.

MATERIALS AND METHODS

Fish maintenance

Zebrafish were maintained under standard conditions at 28.5°C and embryos were obtained by standard breeding methods. All experimental procedures were carried out according to the guidelines of the Institutional Animal Care Use Committee at Temasek Life Sciences Laboratory.

5′ and 3′ RACE

Total RNA was extracted from wild-type embryos and subjected to 5′ and 3′ RACE using the FirstChoice RLM-RACE Kit (Ambion) according to the manufacturer's instructions. The following primers were used: Ints5 5′

[1]Temasek Life Sciences Laboratory, 1 Research Link, National University of Singapore, Singapore 117604. [2]Department of Biological Sciences, 14 Science Drive, National University of Singapore, Singapore 117543. [3]School of Biological Sciences, Nanyang Technological University, 30 Nanyang Drive, Singapore 637551.

*Author for correspondence (e-mail: karuna@tll.org.sg)

Accepted 11 June 2009

RACE, 5′-TCACCCTATGCAGGCCTTGTAGA-3′ and 5′-GGGAGTAGCACTCCATTAGTGA-3′; Ints5 3′ RACE, 5′-GCTACTTCCTCCAGTCTTGAGT-3′ and 5′-CGCTGTGCTATTGCTCTGTCAT-3′. The RACE products were cloned into the plasmid pCS2+ and sequenced.

In situ hybridization analyses

Whole-mount in situ hybridization was performed as described (Tian et al., 2003). The following plasmids were linearized and antisense probes were synthesized by in vitro transcription: pBS*ints5* (*Bam*HI, T3 RNA Polymerase), pGEMT-Easy*scl* (*Nco*I, SP6 RNA Polymerase), pBS*gata1* (*Xba*I, T7 RNA Polymerase), pBS*flk1* (*Sma*I, T7), pKS*pax2a* (*Bam*HI, T7) (Detrich et al., 1995; Gering et al., 1998; Liao et al., 1997; Majumdar et al., 2000), pBS*hgg1* (*Xba*I, T7) (Thisse et al., 1994), pBS*gsc* (*Eco*RI, T7) (Thisse et al., 1994), pBS*ntl* (*Xho*I, T7) (Schulte-Merker et al., 1994), pBS*spt* (*Eco*RI, T7) (Griffin et al., 1998), pBS*sox17* (*Eco*RI, T7) (Alexander and Stainier, 1999), pBS*myoD* (*Bam*HI, T7) (Weinberg et al., 1996) and pBS*dlx3* (*Sal*I, T7) (Akimenko et al., 1994). For digoxigenin- and fluorescein-labeled probes, BM Purple (Roche) and Fast Red (Sigma) substrates were used.

Injection of morpholinos and RNA

All morpholinos were obtained from GeneTools. The *ints5* donor and acceptor morpholinos were designed to target the splice site. Co-injection of the two *ints5* morpholinos (donor and acceptor MO) at an optimal dose of 2.5 ng each was found to have better efficiency, and all injections, unless otherwise specified, were performed using this combination. The *ints11* ATG morpholino was injected at a dose of 25 ng/embryo. The *ints9* SMO targeting the intron2-exon3 boundary of *ints9* was used at a dose of 12.5 ng/embryo. The *ints11* SMO targeting the intron4-exon5 boundary was injected at a dose of 2.5 ng/embryo. The morpholino sequences are: Ints5 donor MO, 5′-CTTGTATTGCTCACCTGTAA-3′; Ints5 acceptor MO, 5′-AGCTCTTGAGGACTGATGGA-3′; Ints9 SMO, 5′-GATAATCGTGGACTGTAAATCCAAC-3′; Ints11 ATG MO, 5′-AAGGCGTAACTTTGATATCAGGCAT-3′; Ints11 SMO, 5′-AGATGGAAATGACTGAGAGGAAGAG-3′. cDNAs encoding Ints5, Ints9, Ints11, Smad1 and Smad5 were cloned in pCS2+. For injection, constructs were digested with *Not*I and the capped mRNA was synthesized with the mMESSAGE mMACHINE SP6 Kit (Ambion) according to the manufacturer's instructions. For rescue experiments, 50 pg of *ints5* RNA or 10 pg of *smad1* and *smad5* RNA was co-injected with *ints5* morpholinos.

RT-PCR

Total RNA from injected embryos (1 μg) was used to generate cDNA with Superscript II Reverse Transcriptase (Invitrogen) and $p(dT)_{15}$ or random $p(dN)_6$ primers (Roche). The cDNA was then used in a PCR reaction. Primer details are available upon request.

May-Grunwald Giemsa staining

Fish embryos were anesthetized in PBS (pH 7.4, calcium- and magnesium-free) with 0.02% tricane (Sigma) and 1% BSA. After tail clipping, red blood cells were collected and cytospun onto slides by centrifugation at 400 rpm for 3 minutes using a Cytospin 4 Cytocentrifuge (Thermo Scientific). The slides were air-dried and subjected to May-Grunwald Giemsa staining (Qian et al., 2007).

Smad cDNA constructs

Smad5Δexon4 and Smad5Δexon4,5 were generated by PCR amplification from cDNA templates (Dick et al., 1999) using the following primers: Smad5Δexon4 F, 5′-CACTACAAACGAGTTGAAAGTCCAGCTGATACTCCTCCTCCTGCCTACAT-3′; Smad5Δexon4 R, 5′-ATGTAGGCAGGAGGAGGAGTATCAGCTGGACTTTCAACTCGTTTGTAGTG-3′; Smad5Δexon4,5 F, 5′-CACTACAAACGAGTTGAAAGTCCAGATGTGCAGCCAGTGGAGTATCAGGA-3′; Smad5Δexon4,5 R, 5′-TCCTGATACTCCACTGGCTGCACATCTGGACTTTCAACTCGTTTGTAGTG-3′. Constructs were linearized with *Not*I and capped mRNA was synthesized with the mMESSAGE mMACHINE SP6 Kit (Ambion).

Quantitative real-time PCR

First-strand cDNA was synthesized using Superscript II Reverse Transcriptase (Invitrogen). Semi-quantitative real-time PCR was performed with the Power SYBR Green PCR Mix (Applied Biosystems) on the

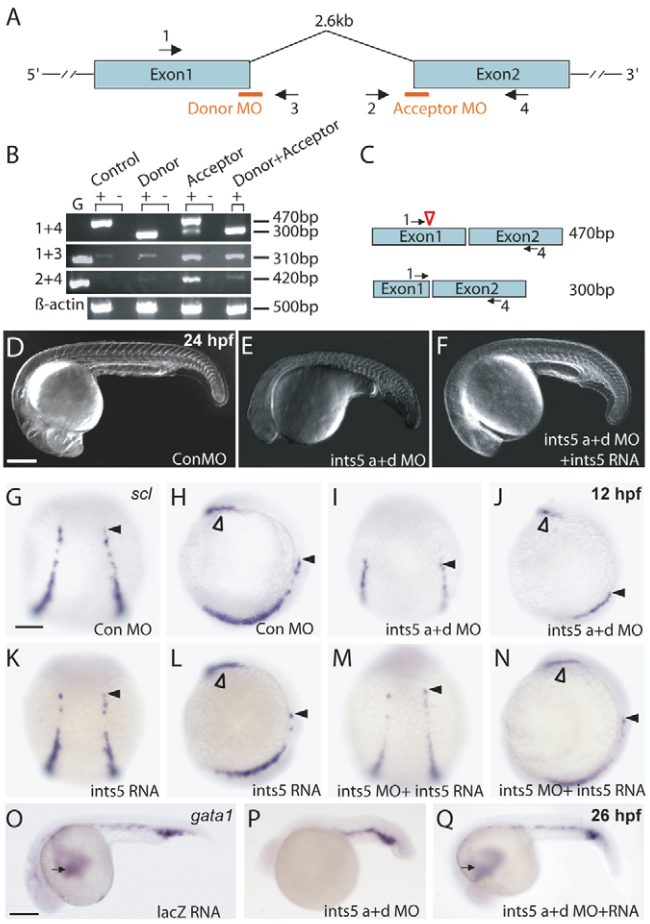

Fig. 1. Ints5 functions during hematopoiesis. (**A**) Schematic representation of the *ints5* genomic locus; orange bars indicate target sites of the donor and acceptor morpholinos (MOs); numbered black arrows show the position of the primers used in RT-PCRs to examine splicing of *ints5* RNA. (**B**) RT-PCR to detect splicing of *ints5* and control β-actin (encoded by *bactin1*). RNA from sphere stage (4 hours post fertilization, hpf) embryos injected with control or *ints5* donor and acceptor morpholinos at the 1-cell stage. Primers used (left) and transcript sizes (right) are indicated. G, genomic DNA. (**C**) Schematic representation of correctly spliced (upper) and aberrantly spliced (lower) *ints5* transcripts. The size of bands amplified by primer pair 1 and 4 is indicated on the right. Red open arrowhead indicates the position of a cryptic splice site in exon 1. (**D-F**) DIC images of live embryos at 24 hpf injected with control morpholinos (D), *ints5* acceptor and donor (a+d) morpholinos (E) or co-injected with *ints5* morpholinos and *ints5* RNA (F). (**G-Q**) Whole-mount in situ hybridization to detect expression of *scl* (G-N) at 12 hpf and *gata1* (O-Q) at 26 hpf shows reduced expression of both genes in *ints5* morphants (I,J,P), in comparison to control morpholino- or *lacZ* RNA-injected embryos (G,H,O). Black arrowheads indicate the anterior limit of *scl* expression in the intermediate cell mass (ICM); open arrowheads indicate *scl* expression in the rostral blood island (RBI); black arrows indicate anterior *gata1* expression, which represents the circulating blood cells. Co-injection of *ints5* RNA can restore *scl* and *gata1* expression in *ints5* morphants (M,N,Q), whereas embryos injected with *ints5* RNA alone show normal *scl* expression at 12 hpf (K,L). D-F,O-Q show lateral views of embryos with anterior to the left; G,I,K,M show dorsal views of embryos with anterior at the top; H,J,L,N show lateral views of embryos with dorsal to the right. Scale bars: 250 μm in D,O; 50 μm in G.

7900HT Fast Real-Time PCR System (Applied Biosystems). Each PCR reaction was performed in triplicate, and each experiment was repeated three times. The PCR cycle conditions were 95°C, 10 minutes and then 94°C, 15 seconds; 60°C, 1 minute, for 45 cycles. The CT values were analyzed using the 2-ΔΔT method. Primer details are available upon request.

Western blots

Western blots were performed on extracts of embryos after removing the yolk. Proteins of each sample were harvested from 20 injected embryos at 8 hpf, separated using SDS-PAGE and transferred to a nitrocellulose membrane (Amersham Biosciences, RPN203E). Ints5 proteins were detected using rabbit anti-Ints5 antibody (1:1000, Bethyl Laboratories). Smad5 proteins were detected using rabbit anti-Smad5 polyclonal antibody (1:500, Abcam). The expression of the α-Tubulin control was detected using anti-α-Tubulin antibody (1:1000, Sigma). Anti-mouse immunoglobulins (1:5000, DAKO) or anti-rabbit immunoglobulins (1:5000, DAKO) were used as secondary antibodies and were detected with SuperSignal West Femto Maximum Sensitivity Substrate (Pierce) or with SuperSignal West Pico Chemiluminescent Substrate (Pierce).

RESULTS

Ints5 functions during primitive hematopoiesis.

To investigate the function of Ints5 during early zebrafish development, two antisense morpholinos were designed to target the intronic donor and acceptor sites of the *ints5* gene (Fig. 1A). Reverse transcription-PCR (RT-PCR) analysis shows the accumulation of nonspliced *ints5* transcripts in embryos injected with *ints5* splice-junction morpholinos (Fig. 1B). Sequence analysis of RT-PCR products from the transcripts shows that the correct exon-intron boundary is not chosen and, instead, a cryptic site in exon 1 of *ints5* is used in the morphant embryos. This leads to the production of

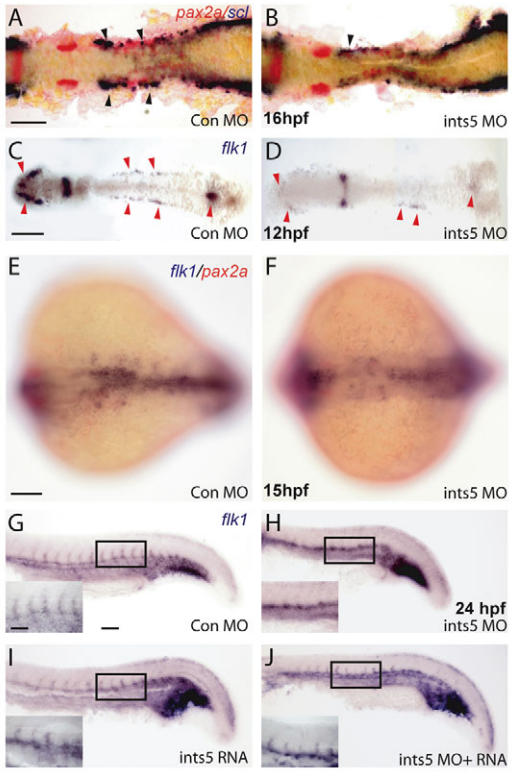

Fig. 2. Ints5 knockdown affects hematopoietic progenitors but not pronephric cells. (**A-F**) In situ hybridization to detect expression of *scl* (purple) in hematopoietic cells, *pax2a* (red) in the pronephric cells and *flk1* (purple) in endothelial cells. (A,B) *scl* and *pax2a* expression in control (A) and *ints5* morphants (B) at 16 hpf. Black arrowheads indicate the anterior *scl* expression in the ICM, and its reduction in *ints5* morphants; *pax2a* expression is unaffected. (C-F) Expression of *flk1* in control (C,E) and *ints5* morphants (D,F) at 12 hpf (C,D) and 15 hpf (E,F). Red arrowheads indicate *flk1* expression, which is much reduced in *ints5* morphants at an early stage (C,D) but recovers later in development (E,F). (**G-J**) Expression of *flk1* in injected embryos at 24 hpf. Insets show enlarged views of the boxed areas. Inter-segmental *flk1* expression is not detected in *ints5* morphants (H), in comparison to control embryos (G) and *ints5* RNA-injected embryos (I). Expression of *flk1* in inter-segmental vessels is rescued by co-injection of *ints5* RNA (J). A-D show dorsal views of flat-mounted embryos; E,F show dorsal views with anterior to the left; G-J show lateral views of the trunk with anterior to the left. Scale bars: 100 μm in A,C,E,G; 50 μm in inset in G.

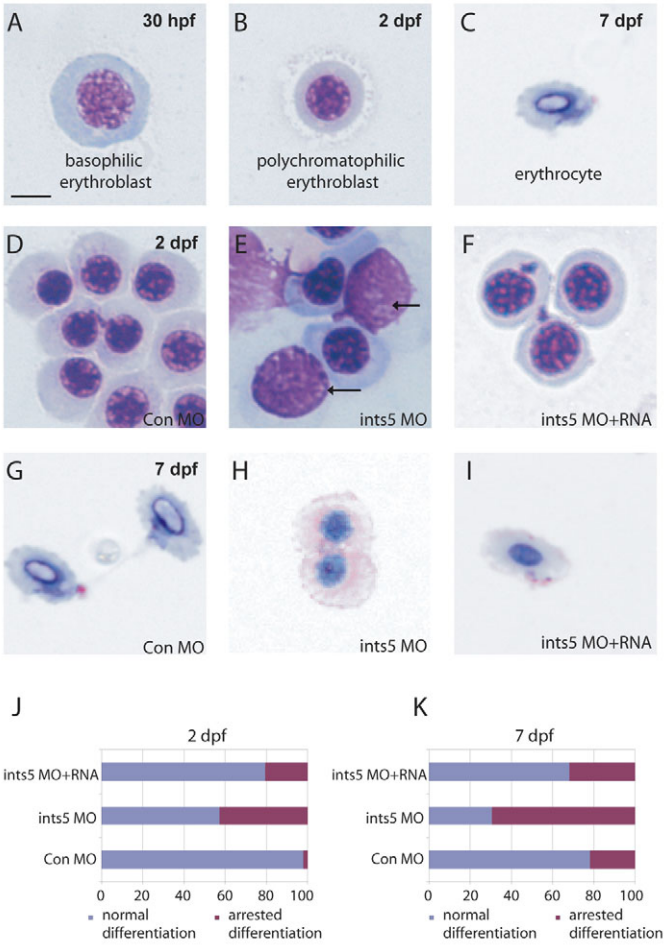

Fig. 3. Ints5 is required for erythrocyte differentiation. (**A-C**) May-Grunwald Giemsa staining shows normal red blood cells (RBCs) at various stages of differentiation at the indicated embryonic stages. (**D-F**) RBCs in embryos injected with control morpholinos (D), *ints5* morpholinos (E), or co-injected with *ints5* RNA and morpholinos (F) at 2 dpf. Arrows indicate the RBCs arrested at the basophilic erythroblast stage (E). (**G-I**) RBCs in embryos injected with control morpholinos (G), *ints5* morpholinos (H), or co-injected with *ints5* RNA and morpholinos (I) at 7 dpf. (**J**,**K**) Histograms showing the percentage of RBCs with normal (blue) or arrested (magenta) differentiation in injected embryos at 2 dpf (J) and 7 dpf (K). Scale bar: 10 μm.

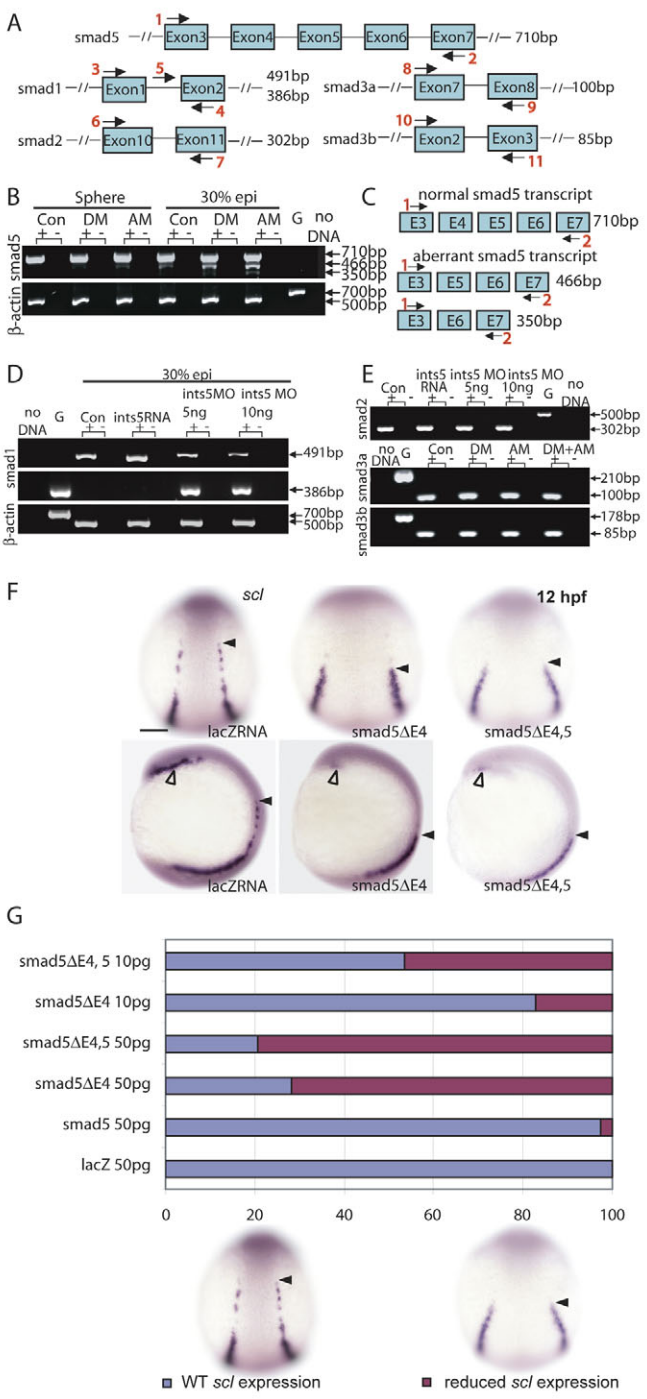

Fig. 4. Knockdown of Ints5 perturbs splicing of *smad1* and *smad5* RNA. (**A**) Schematic representation of the *smad5*, *smad1*, *smad2*, *smad3a* and *smad3b* genomic loci. Numbered black arrows indicate the position of primers used in RT-PCRs to detect splicing. The sizes of the predicted products using various primer pairs are indicated on the right. (**B**) At both sphere and 30% epiboly stages, aberrantly spliced *smad5* transcripts accumulate in *ints5* donor morpholino (DM)- and acceptor mopholino (AM)-injected embryos. β-actin control transcripts are correctly spliced to yield a 500 bp product from cDNA in comparison to a 700 bp genomic DNA product, G. (**C**) Schematic representation to show the wild-type 710 bp *smad5* transcript, and aberrant *smad5* transcripts that lack exon 4 (466 bp product), or lack both exon 4 and exon 5 (350 bp product). (**D**) Unspliced *smad1* (386 bp product with primer pair 4 and 5) and correctly spliced *smad1* (491 bp with primer pair 3 and 4) transcripts in 30% epiboly *ints5* morpholino-injected embryos. (**E**) Amplification of *smad2*, *smad3a* and *smad3b* with the primer pairs indicated in A shows correctly spliced products in *ints5* morphants. Amplification with primers spanning other regions of these genes also did not show aberrant splicing (data not shown). (**F**,**G**) Overexpression of truncated *smad5* transcripts causes hematopoiesis defects, similar to *ints5* morphants. (F) Whole-mount in situ hybridization to detect *scl* in control embryos (left), and in embryos injected with *smad5ΔE4* RNA (middle) or *smad5ΔE4,5* RNA (right) at 12 hpf. Black arrowheads indicate the anterior limit of *scl* expression in the ICM; open arrowheads mark *scl* expression in the RBI. Upper panel shows dorsal views with anterior to the top; lower panel shows lateral views with dorsal to the right. (G) Histogram showing the percentage of injected embryos with wild-type (blue) or reduced (magenta) *scl* expression levels. Scale bar: 50 μm.

incorrectly spliced *ints5* transcripts lacking 170 bp of the coding sequence (Fig. 1C). Western blot analysis using antibodies to detect Ints5 protein in embryo extracts shows that the *ints5* morpholinos disrupt the synthesis of Ints5 proteins (see Fig. S1 in the supplementary material).

By 24 hpf, embryos injected with *ints5* splice-junction morpholinos showed severe defects, with a shortened anterior-posterior axis and no circulating blood cells (Fig. 1E,P), in comparison to control morpholino- or RNA-injected embryos (Fig. 1D,O), indicating defects in convergent-extension cell movement and hematopoiesis. These phenotypes were rescued by co-injecting *ints5* RNA with the *ints5* splice-junction morpholinos (Fig. 1F,Q).

To determine if specification of the germ layers is affected in the *ints5* morphant embryos, we examined the expression of various germ-layer and cell-type specific marker genes during gastrulation (see Figs S2 and S7 in the supplementary material). Analysis of the expression of *ntl* (*ntla* – ZFIN) and *spt* (*tbx16* – ZFIN) in the mesoderm, *gsc* in the dorsal organizer, *dlx3* (*dlx3b* – ZFIN) in the neural plate, *sox17* in the endoderm and *myoD* (*myod1* – ZFIN) in the myotome showed that knockdown of *ints5* does not affect germ-layer specification. Furthermore, the patterning of dorsoventral and anterior-posterior axes was largely normal, and the shortened axis in *ints5* morphant embryos is therefore likely to be a result of impaired convergent-extension cell movements.

Since blood circulation is impaired in *ints5* morphants, we examined the expression of the hematopoietic genes *stem cell leukemia* (*scl*) and *gata1* by whole-mount in situ hybridization. The expression of *scl* transcripts was severely reduced in *ints5* morphants (Fig. 1I,J; Fig. 2B; see Fig. S7B in the supplementary material) in comparison to control embryos (Fig. 1G,H; Fig. 2A; see Fig. S7A in the supplementary material). By contrast, the adjacent *pax2a*-expressing pronephric cells were not affected in *ints5* morphants (Fig. 2A,B) (Majumdar et al., 2000). The expression of *gata1*, which is crucial for the specification of erythrocytes, was also reduced in *ints5* morphants (Fig. 1P) (Orkin and Zon, 1997). This reduction is rescued by the co-injection of *ints5* RNA (Fig. 1M,N,Q), whereas overexpression of *ints5* RNA by itself does not affect *scl* or *gata1* expression (Fig. 1K,L; data not shown). Semi-quantitative RT-PCR to determine the levels of *scl* and *gata1* RNA also show reduced expression of these genes in *ints5* morphants (see Fig. S3A,B in the supplementary material), which is rescued by co-injection of *ints5* RNA. Together, these experiments show that Ints5 function is required during primitive hematopoiesis.

As *scl* expression is also crucial for the formation of vascular precursors, we examined the expression of the endothelial gene *flk1* (*kdrl* – ZFIN) at various stages (de Jong and Zon, 2005; Liao et al., 1997). We find that, although the early expression of *flk1* is reduced in *ints5* morphants (Fig. 2C,D; see Fig. S3C in the supplementary material), this seems to recover later, and by 24 hpf, with the exception of the inter-segmental vessels, *flk1* expression is detected in most domains observed in control embryos (Fig. 2E-J). The lack of *flk1* expression in inter-segmental vessels might reflect cell migration and/or vessel branching defects. These results suggest that the common progenitor of hematopoietic and endothelial cells, the hemangioblast precursors (Vogeli et al., 2006), are not affected in *ints5* morphants per se, and that Ints5 function is required for hematopoietic development.

Ints5 is required for erythrocyte differentiation

A previous study by Qian et al. (Qian et al., 2007) showed that *scl* isoforms function in the initiation of primitive hematopoiesis and regulate erythroid cell differentiation. Since *ints5* morpholino-injected embryos have reduced *scl* expression, we examined erythroid differentiation in Ints5-manipulated embryos. May-Grunwald Giemsa staining of blood smears from wild-type embryos revealed normal erythrocyte progenitors. These cells differentiate and are typically categorized as: stage I, basophilic erythroblast (30 hpf); stage II, polychromatophilic erythroblast (2 days post fertilization, dpf); stage III, orthochromatophilic erythroblast (4 dpf); stage IV, erythrocyte (5 dpf onwards) (Fig. 3A-C; data not shown), based on the shape of their nucleus, size and morphology of the cells, and staining of the cytoplasm (Qian et al., 2007).

Blood smear analysis showed that, whereas 98% of RBCs grow to the polychromatophilic erythroblast stage (stage II) in control embryos by 2 dpf (Fig. 3D,J), only 58% of RBCs in *ints5* morphants develop normally. In *ints5* morphant embryos, 42% of cells arrested at the basophilic erythroblast stage (stage I; Fig. 3E,J). To investigate the role of Ints5 in RBC differentiation, we reduced the dosage of the antisense morpholinos so as to allow embryos to survive to later stages. At 7 dpf, only 30% of RBCs in *ints5* morphant embryos differentiated normally in comparison to control embryos in which ~80% of the cells are fully developed mature RBCs with flattened elliptical shape (Fig. 3G,H,K). Normal differentiation of RBCs in *ints5* morphants was restored by co-injection of *ints5* RNA (Fig. 3F,I,J,K). Thus, Ints5 function is required for the differentiation of erythrocytes.

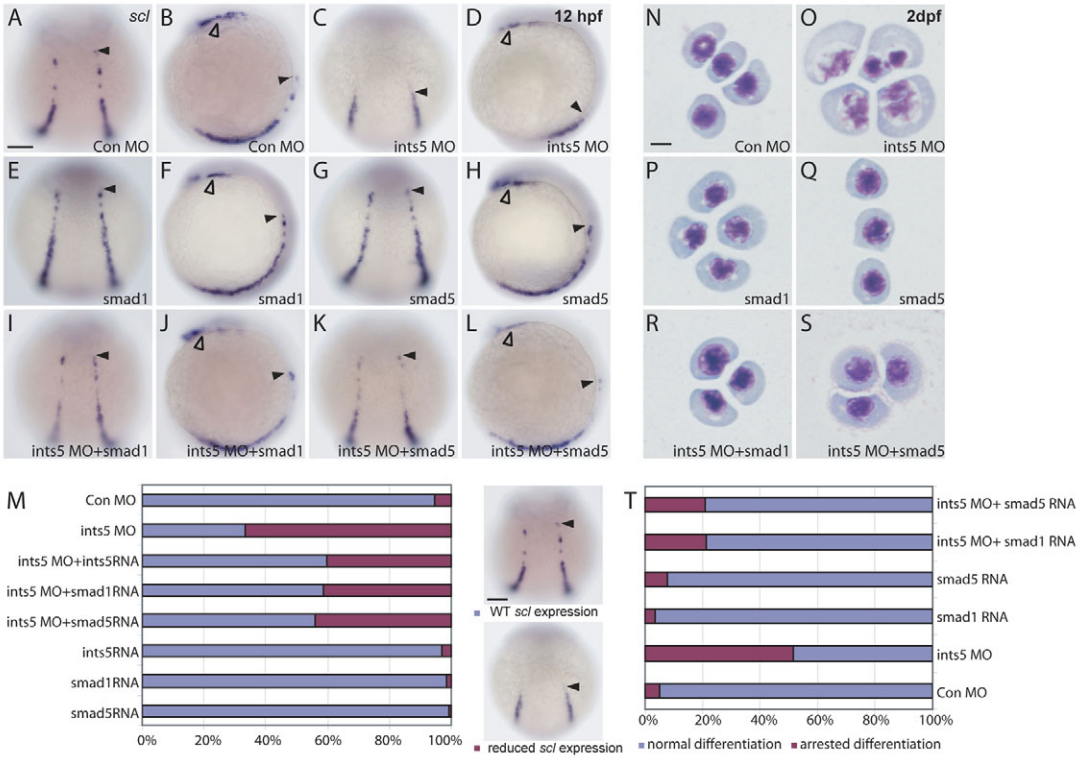

Fig. 5. The hematopoiesis defects induced by Ints5 knockdown are rescued by *smad1* and *smad5* RNA. (**A-L**) Whole-mount in situ hybridization to detect *scl* expression in 12 hpf embryos injected with control morpholinos (A,B), *ints5* morpholinos (C,D), *smad1* RNA (E,F), *smad5* RNA (G,H), *ints5* morpholinos with *smad1* RNA (I,J), or *ints5* morpholinos with *smad5* RNA (K,L). Black arrowheads indicate the anterior limit of *scl* expression in the ICM; open arrowheads indicate *scl* expression in the RBI. A,C,E,G,I,K show dorsal views of embryos with anterior to the top; B,D,F,H,J,L show lateral views of embryos with dorsal to the right. (**M**) Histogram showing the percentage of injected embryos with wild-type-like (blue) or reduced (magenta) *scl* expression. The total number of embryos for each staining is >180, and all experiments were carried out three independent times (see Table S1 in the supplementary material). (**N-S**) May-Grunwald Giemsa staining to show RBC differentiation in embryos injected with control morpholinos (N), *ints5* morpholinos (O), *smad1* RNA (P), *smad5* RNA (Q), *ints5* morpholinos with *smad1* RNA (R), or *ints5* morpholinos with *smad5* RNA (S) at 2 dpf. (**T**) Histogram showing the percentage of RBCs with normal (blue) or arrested (magenta) differentiation in injected embryos at 2 dpf. The total number of red blood cells counted for each sample is >200, and all experiments were carried out three independent times. Scale bars: 50 μm in A,M; 10 μm in N.

Ints5 is necessary for splicing of *smad1* and *smad5* transcripts

The Integrator complex is thought to be involved in snRNA processing (Baillat et al., 2005). As *ints5* morpholino-injected embryos have decreased *scl* expression, similar to *smad5* mutant embryos (McReynolds et al., 2007), we investigated whether the splicing of *smad5* and *smad1* is disrupted in *ints5* morphant embryos. Splicing of *smad2*, *smad3a*, *smad3b*, *cyclops* (*ndr2* – ZFIN), *squint* (*ndr1* – ZFIN) and actin (*bactin1* – ZFIN) RNAs was also examined as controls. Total RNA was extracted from embryos injected with control or *ints5* splice morpholinos, and RT-PCR was performed with primers for the various genes (Fig. 4A). In *ints5* morpholino-injected embryos, as early as gastrula stages we detected significant amounts of aberrantly spliced *smad5* transcripts that either lacked exon 4 or both exon 4 and exon 5 (Fig. 4B,C). To test the activity of the aberrant *smad5* splice products, we overexpressed capped synthetic mRNA encoding Smad5 lacking exon 4 (*smad5Δexon4*), or exons 4 and 5 (*smad5Δexon4,5*). Analysis of *scl* expression showed that embryos injected with *smad5Δexon4* or *smad5Δexon4,5* RNA have reduced expression, similar to *ints5* morphants (Fig. 4F,G). Furthermore, western blot analysis using antibodies to detect Smad5 protein in embryo extracts showed that the *ints5* morpholinos disrupted the synthesis of Smad5 proteins and led to the accumulation of truncated Smad5 proteins. The truncated Smad5 proteins correspond to proteins encoded by the aberrant transcripts, *smad5Δexon4* and *smad5Δexon4,5* (see Fig. S4 in the supplementary material). These truncated proteins might function as dominant-negative peptides that disrupt Smad5 function during development.

Similarly, unspliced *smad1* transcripts are also detected in *ints5* morpholino-injected embryos (Fig. 4D). However, we did not observe aberrant splicing of any exon-intron boundary of *smad2*, *smad3a* or *smad3b* transcripts, or other examined transcripts (Fig. 4E; see Fig. S5 in the supplementary material; data not shown). These results show that Ints5 is specifically required for the correct splicing of *smad1* and *smad5* RNA.

To understand the mechanism underlying the *smad1/5* splicing defects in *ints5* morphants, we examined the expression and processing of U1/U2 snRNA (see Fig. S6A in the supplementary material). Semi-quantitative RT-PCR analysis showed an accumulation of unprocessed primary U1/U2 snRNAs in *ints5* morpholino-injected embryos (see Fig. S6B,C,D in the supplementary material). In contrast to the increased primary U1/U2 snRNAs, the level of mature U1/U2 snRNAs was not significantly altered in *ints5* morphants (see Fig. S6E,F in the supplementary material). These results show that Ints5 regulation of *smad1/5* RNA splicing is mediated via U1/U2 snRNA processing.

Ints5 modulates hematopoiesis through Smad/BMP signaling

To determine the epistatic relationship between Ints5 and Smad1 or Smad5, we injected 10 pg of capped *smad1* or *smad5* RNA together with *ints5* morpholinos into 1-cell-stage embryos. We found that co-injected *smad1* or *smad5* RNA could restore *scl* expression and RBC differentiation in *ints5* morphants, similar to *ints5* RNA co-injections (Fig. 5C,D,I-L,M,O,R,S,T; see Fig. S7B,E,F in the supplementary material; see Table S1 in the supplementary material; $P \ll 0.01$). Control embryos injected with 10 pg of *smad1* or *smad5* RNA alone showed normal *scl* expression and RBC differentiation (Fig. 5E-H,M,P,Q,T; see Fig. S7C,D in the supplementary material), similar to those injected with control morpholinos (Fig. 5A,B,M,N,T; see Fig. S7A in the supplementary material). Blood circulation was also restored in *ints5* morphants upon rescue with *smad1* or *smad5* RNA (data not shown). These results, together with

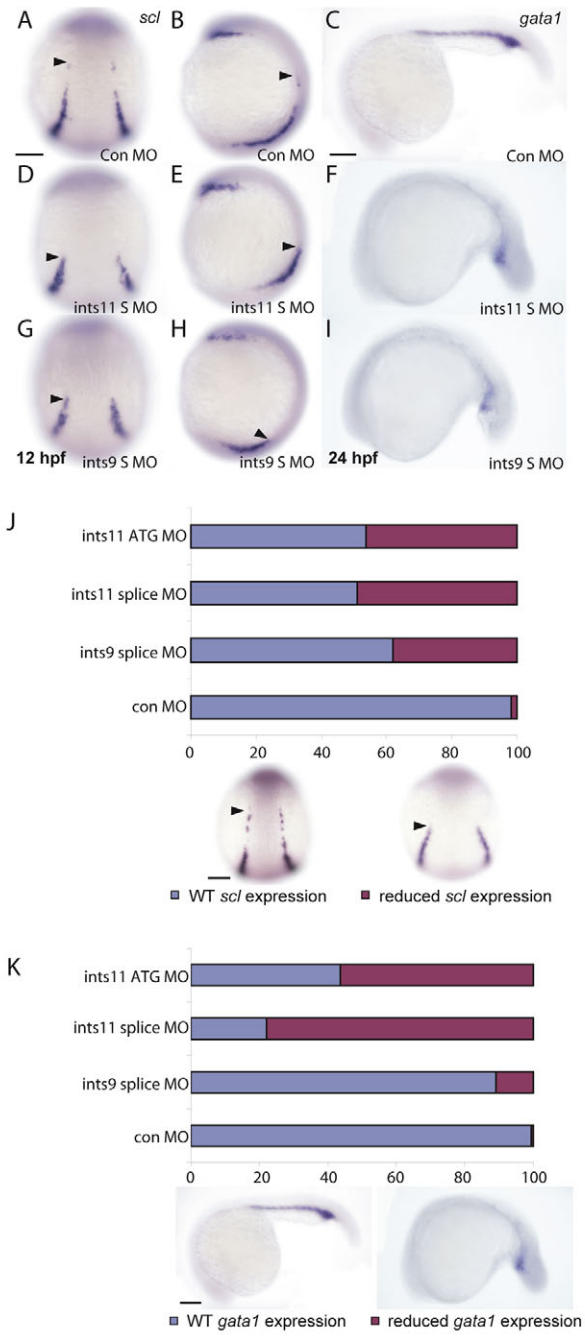

Fig. 6. Multiple subunits of the Integrator complex regulate primitive hematopoiesis. (**A-I**) Whole-mount in situ hybridization to detect *scl* (A,B,D,E,G,H) and *gata1* (C,F,I) expression in embryo injected with control morpholinos (A-C), *ints11* splice-junction morpholinos (S MO, D-F) and *ints9* splice-junction morpholinos (G-I). Black arrowhead indicates the anterior limit of *scl* expression in the ICM. The *ints9* and *ints11* morphants show substantially reduced *scl* and *gata1* expression in comparison to control morphants. (**J**,**K**) Histograms showing the percentage of injected embryos with wild-type (blue) or reduced (magenta) *scl* (J) and *gata1* (K) expression levels. Scale bars: 50 μm in A,J; 250 μm in C,K.

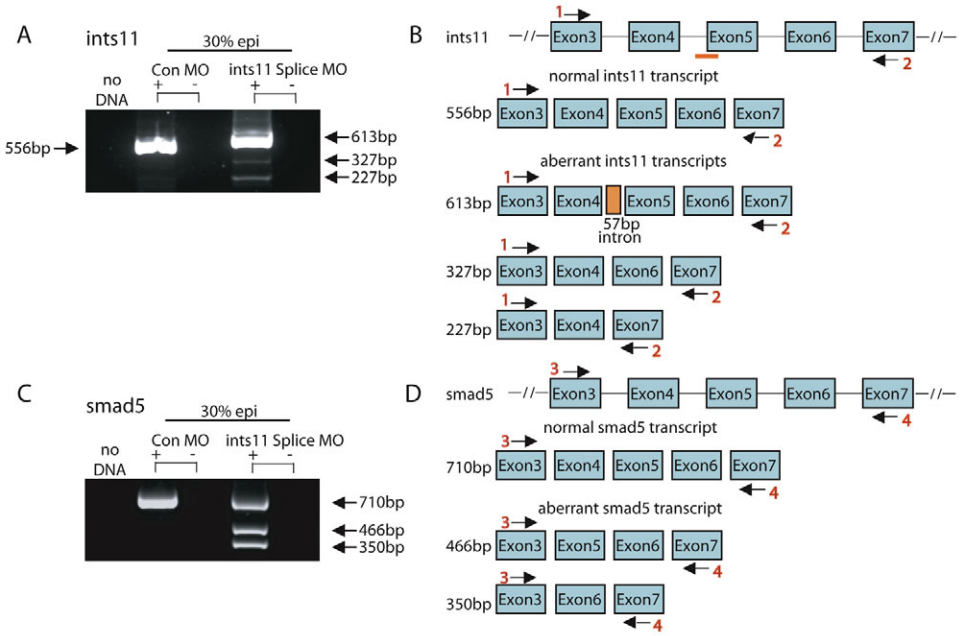

Fig. 7. Knockdown of *ints11* perturbs *smad5* splicing. (**A**) RT-PCR analysis shows that the *ints11* splice-junction morpholino efficiently blocks the correct splicing of *ints11* RNA, and several aberrant transcripts are detected. Transcripts are indicated by black arrows, with sizes indicated. (**B**) Schematic representation of the *ints11* genomic locus (upper panel); schematic representation of normal or aberrant *ints11* transcripts is shown in the lower panel. Numbered black arrows indicate the position of primers used in RT-PCRs to detect splicing. Orange bar shows the target site of the *ints11* splice-site morpholino. (**C**) RT-PCR analysis shows that splicing of *smad5* is impaired in *ints11* morphants. (**D**) Schematic representation of the *smad5* genomic locus (upper panel); the lower panel shows schematic representations of normal and aberrantly spliced *smad5* transcripts.

the results from semi-quantitative RT-PCR experiments (see Fig. S3 in the supplementary material), show that Ints5 functions in hematopoiesis by modulating *smad1/5* RNA splicing.

The Integrator complex regulates primitive hematopoiesis

As Ints5 is a subunit of the Integrator complex (Baillat et al., 2005), to find out whether Ints5 functions independently or as part of the Integrator complex in regulating hematopoiesis, we examined the activity of other Integrator subunits. We injected *ints11* (*zgc::110671* – ZFIN) ATG morpholinos and splice morpholinos targeting the boundary of intron 4 and exon 5 in the *ints11* gene into 1-cell-stage embryos. Both *ints11* morpholinos caused reduced expression of the hematopoietic markers *scl* and *gata1* (Fig. 6A-C,D-F,J,K; data not shown) in more than 50% embryos. In addition, embryos injected with *ints9* (*zgc::154012* – ZFIN) splice morpholinos targeting the boundary of intron 2 and exon 3 showed similar hematopoiesis defects (Fig. 6G-K). Morpholinos targeting the splice junction of *ints11* also caused defects in *smad5* splicing, U1/U2 snRNA processing and hematopoiesis (Figs 6 and 7; see Fig. S6B in the supplementary material). Therefore, multiple subunits of the Integrator complex, including Ints5, might be required for appropriate hematopoietic gene expression. These results suggest that the Integrator proteins function as a complex to regulate primitive hematopoiesis by modulating *smad1/5* splicing during zebrafish development.

DISCUSSION

Although hematopoiesis has been extensively studied, the molecular program of hematopoietic stem cell induction and self-renewal remains unclear. Recent work has revealed that the post-transcriptional processing of BMP Smads is involved in the maintenance of hematopoietic stem cell identity. Jiang et al. identified a C-terminal truncation in SMAD5, SMAD5β, which inactivates the protein. SMAD5β is expressed in both normal hematopoiesis and leukemogenesis (Jiang et al., 2000). Interestingly, the expression level of the SMAD5β isoform is higher in CD34+ hematopoietic stem cells than in terminally differentiated peripheral blood leukocytes, indicating that the alternative splicing of *SMAD5* is differentially regulated during the maturation of hematopoietic cells. Our work shows that the splicing of *smad1/5* is impaired by the knockdown of Ints5. Aberrant splicing of *smad5* leads to the production of dominant-negative forms of Smad5, the overexpression of which phenocopies the hematopoiesis phenotypes we observed in *ints5* morphants. These include reduced the expression of *scl* and, eventually, failure in erythrocyte differentiation. Thus, the accurate splicing of *smad5* is crucial for the normal progression of hematopoiesis and erythropoietic differentiation, and the failure to generate appropriate Smad5 products can lead to a reduction of hematopoietic progenitors.

The analysis of germ-layer specification and dorsoventral patterning suggests that these developmental processes are not affected in *ints5* morphant embryos. In addition, the expression of *pax2a*, *spt*, *myoD* and *ntl* suggests that anterior-posterior patterning is also largely normal (Fig. 2B; see Fig. S2F, Fig. S7B and Fig. S9C in the supplementary material). It may seem surprising that, although Ints5 knockdown affects *smad1/5* splicing, we do not observe early dorsoventral or anterior-posterior patterning, or germ-layer specification defects (see Fig. S2 in the supplementary material), as observed for *smad5* and other BMP pathway mutants (Dick et al., 2000; Hild et al., 1999; Kishimoto et al., 1997; Kodjabachian et al., 1999; Mullins et al., 1996; Schmid et al., 2000; Schulte-Merker et al., 1997). This can be explained by the maternal deposition of Integrator complex factors such as Ints5 (see Fig. S8 in the supplementary material). The maternal Ints products might allow normal functioning of the Integrator complex in early embryos, such that the early patterning events that are mediated by BMP signaling are not affected by the knockdown of Ints5. We also observe convergent-extension defects in *ints5* morphants (Fig 1E; see Fig. S2E,F,I,J and Fig. S9C,D,M in the supplementary material), leading to a shortened anterior-posterior axis in *ints5* morphants. It is possible that the Integrator subunits also regulate cell movements via Smad1/5 signaling, as co-injection of *smad1/5* RNA can restore normal cell movements in *ints5* morphants (see Fig. S9I-L,M in the supplementary material).

One interesting question is how the Integrator complex proteins, which are thought to function in RNA processing, might have such a specific effect on Smad/BMP signaling and hematopoiesis. Only *smad1* and *smad5* splicing is affected, whereas the expression of other Smads (e.g. *smad2*, *smad3a* and *smad3b*) is not disrupted, suggesting that the Integrator complex does not generally affect all splicing. Furthermore, our analysis of several genes [*chordin*, *vent*, *vox*, *ved*, *gata2a*, *eve1*, *smurf1* (*wwp1* – ZFIN), *bmp2b*, *bmp7a*, *ski* (*skia* – ZFIN), *sqt*, *cyc* and others] shows that the disruption of Integrator complex function does not generally affect genes expressed during gastrulation. This raises the possibility that the Integrator complex might be functioning specifically in the cells that respond to BMP signaling.

It is now known that mutations affecting some transcription or translation machinery components can have very specific effects on distinct cell types (Pellizzoni, 2007; van der Knaap et al., 2006). Recent work by Watanabe et al. has shown that Sf3b4, a subunit of Sf3b, which is a common RNA splicing complex, specifically binds to Bmpr1a and inhibits BMP signaling during osteochondral cell differentiation (Watanabe et al., 2007). There might be a potential connection between TGFβ/BMP signaling and the RNA processing machinery. So it is possible that Ints5, which is involved in U1/U2 snRNA maturation, which in turn is important for pre-mRNA splicing, might cooperate with other RNA splicing factors in specific cellular contexts (such as in hematopoietic progenitors), to specifically modulate BMP signaling via *smad1/smad5* RNA splicing. Alternatively, Ints5 itself might be post-transcriptionally regulated via factors that are specific to hematopoietic progenitors.

Deficiencies in RNA splicing have been shown to cause many genetic disorders (Pellizzoni, 2007; Solis et al., 2008). As the Integrator complex plays a vital role in the transcription and processing of snRNA, dysfunction of the Integrator subunits can lead to various developmental defects. In fact, recent work has shown that disruption of the murine integrator complex subunit 1 causes growth arrest and eventual apoptosis at early blastocyst stages (Hata and Nakayama, 2007). Integrator subunit 3 is a probable target for the amplification of chromosomal region 1q21 found in most hepatocellular carcinoma (HCC) tumors, and may be involved in the development and/or progression of this cancer (Inagaki et al., 2008). However, it is still unclear how these genes function, and how their malfunction leads to profound defects in specific biological processes. The study presented here reveals a potential link between snRNA processing and BMP signaling in hematopoiesis. Understanding the precise mechanisms by which the individual subunits function may provide insights into the roles played by the Integrator complex during development and tumorigenesis.

Acknowledgements

We thank Aniket Gore, Roland Dosch, Yun-Jin Jiang and members of the Sampath laboratory for discussions and suggestions; Helen Ngoc Bao Quach, Jiang Guanying and Leong Li Sun for technical assistance; Qian Feng for advice on blood smear analysis; Ge Ruowen for the *flk1* construct; and the TLL fish facility and sequencing facility. Work in the laboratory of Karuna Sampath is supported by the Temasek Life Sciences Laboratory, Singapore.

Competing interest statement

The authors have no competing interests.

Supplementary material

Supplementary material for this article is available at http://dev.biologists.org/cgi/content/full/136/16/2757/DC1

References

Akimenko, M. A., Ekker, M., Wegner, J., Lin, W. and Westerfield, M. (1994). Combinatorial expression of three zebrafish genes related to distal-less: part of a homeobox gene code for the head. *J. Neurosci.* **14**, 3475-3486.

Al-Adhami, M. A. and Kunz, Y. W. (1977). Ontogenesis of Hematopoietic sites in Brachydanio rerio. *Dev. Growth Differ.* **19**, 171-179.

Alexander, J. and Stainier, D. Y. (1999). A molecular pathway leading to endoderm formation in zebrafish. *Curr. Biol.* **9**, 1147-1157.

Baillat, D., Hakimi, M. A., Naar, A. M., Shilatifard, A., Cooch, N. and Shiekhattar, R. (2005). Integrator, a multiprotein mediator of small nuclear RNA processing, associates with the C-terminal repeat of RNA polymerase II. *Cell* **123**, 265-276.

Davidson, A. J. and Zon, L. I. (2004). The 'definitive' (and 'primitive') guide to zebrafish hematopoiesis. *Oncogene* **23**, 7233-7246.

de Jong, J. L. and Zon, L. I. (2005). Use of the zebrafish system to study primitive and definitive hematopoiesis. *Annu. Rev. Genet.* **39**, 481-501.

Detrich, H. W., 3rd, Kieran, M. W., Chan, F. Y., Barone, L. M., Yee, K., Rundstadler, J. A., Pratt, S., Ransom, D. and Zon, L. I. (1995). Intraembryonic hematopoietic cell migration during vertebrate development. *Proc. Natl. Acad. Sci. USA* **92**, 10713-10717.

Dick, A., Meier, A. and Hammerschmidt, M. (1999). Smad1 and Smad5 have distinct roles during dorsoventral patterning of the zebrafish embryo. *Dev. Dyn.* **216**, 285-298.

Dick, A., Hild, M., Bauer, H., Imai, Y., Maifeld, H., Schier, A. F., Talbot, W. S., Bouwmeester, T. and Hammerschmidt, M. (2000). Essential role of Bmp7 (snailhouse) and its prodomain in dorsoventral patterning of the zebrafish embryo. *Development* **127**, 343-354.

Fehling, H. J., Lacaud, G., Kubo, A., Kennedy, M., Robertson, S., Keller, G. and Kouskoff, V. (2003). Tracking mesoderm induction and its specification to the hemangioblast during embryonic stem cell differentiation. *Development* **130**, 4217-4227.

Gering, M., Rodaway, A. R., Gottgens, B., Patient, R. K. and Green, A. R. (1998). The SCL gene specifies haemangioblast development from early mesoderm. *EMBO J.* **17**, 4029-4045.

Griffin, K. J., Amacher, S. L., Kimmel, C. B. and Kimelman, D. (1998). Molecular identification of spadetail: regulation of zebrafish trunk and tail mesoderm formation by T-box genes. *Development* **125**, 3379-3388.

Hata, T. and Nakayama, M. (2007). Targeted disruption of the murine large nuclear KIAA1440/Ints1 protein causes growth arrest in early blastocyst stage embryos and eventual apoptotic cell death. *Biochim. Biophys. Acta* **1773**, 1039-1051.

Hild, M., Dick, A., Rauch, G. J., Meier, A., Bouwmeester, T., Haffter, P. and Hammerschmidt, M. (1999). The smad5 mutation somitabun blocks Bmp2b signaling during early dorsoventral patterning of the zebrafish embryo. *Development* **126**, 2149-2159.

Hsu, K., Kanki, J. P. and Look, A. T. (2001). Zebrafish myelopoiesis and blood cell development. *Curr. Opin. Hematol.* **8**, 245-251.

Inagaki, Y., Yasui, K., Endo, M., Nakajima, T., Zen, K., Tsuji, K., Minami, M., Tanaka, S., Taniwaki, M., Itoh, Y. et al. (2008). CREB3L4, INTS3, and SNAPAP are targets for the 1q21 amplicon frequently detected in hepatocellular carcinoma. *Cancer Genet. Cytogenet.* **180**, 30-36.

Jiang, Y., Liang, H., Guo, W., Kottickal, L. V. and Nagarajan, L. (2000). Differential expression of a novel C-terminally truncated splice form of SMAD5 in hematopoietic stem cells and leukemia. *Blood* **95**, 3945-3950.

Kishimoto, Y., Lee, K. H., Zon, L., Hammerschmidt, M. and Schulte-Merker, S. (1997). The molecular nature of zebrafish swirl: BMP2 function is essential during early dorsoventral patterning. *Development* **124**, 4457-4466.

Kodjabachian, L., Dawid, I. B. and Toyama, R. (1999). Gastrulation in zebrafish: what mutants teach us. *Dev. Biol.* **213**, 231-245.

Larsson, J. and Karlsson, S. (2005). The role of Smad signaling in hematopoiesis. *Oncogene* **24**, 5676-5692.

Liao, W., Bisgrove, B. W., Sawyer, H., Hug, B., Bell, B., Peters, K., Grunwald, D. J. and Stainier, D. Y. (1997). The zebrafish gene cloche acts upstream of a flk-1 homologue to regulate endothelial cell differentiation. *Development* **124**, 381-389.

Majumdar, A., Lun, K., Brand, M. and Drummond, I. A. (2000). Zebrafish no isthmus reveals a role for pax2.1 in tubule differentiation and patterning events in the pronephric primordia. *Development* **127**, 2089-2098.

McReynolds, L. J., Gupta, S., Figueroa, M. E., Mullins, M. C. and Evans, T. (2007). Smad1 and Smad5 differentially regulate embryonic hematopoiesis. *Blood* **110**, 3881-3890.

Mullins, M. C., Hammerschmidt, M., Kane, D. A., Odenthal, J., Brand, M., van Eeden, F. J., Furutani-Seiki, M., Granato, M., Haffter, P., Heisenberg, C. P. et al. (1996). Genes establishing dorsoventral pattern formation in the zebrafish embryo: the ventral specifying genes. *Development* **123**, 81-93.

Orkin, S. H. and Zon, L. I. (1997). Genetics of erythropoiesis: induced mutations in mice and zebrafish. *Annu. Rev. Genet.* **31**, 33-60.

Pellizzoni, L. (2007). Chaperoning ribonucleoprotein biogenesis in health and disease. *EMBO Rep.* **8**, 340-345.

Qian, F., Zhen, F., Xu, J., Huang, M., Li, W. and Wen, Z. (2007). Distinct functions for different scl isoforms in zebrafish primitive and definitive hematopoiesis. *PLoS Biol.* **5**, e132.
Schmid, B., Furthauer, M., Connors, S. A., Trout, J., Thisse, B., Thisse, C. and Mullins, M. C. (2000). Equivalent genetic roles for bmp7/snailhouse and bmp2b/swirl in dorsoventral pattern formation. *Development* **127**, 957-967.
Schulte-Merker, S., van Eeden, F. J., Halpern, M. E., Kimmel, C. B. and Nusslein-Volhard, C. (1994). no tail (ntl) is the zebrafish homologue of the mouse T (Brachyury) gene. *Development* **120**, 1009-1015.
Schulte-Merker, S., Lee, K. J., McMahon, A. P. and Hammerschmidt, M. (1997). The zebrafish organizer requires chordino. *Nature* **387**, 862-863.
Solis, A. S., Shariat, N. and Patton, J. G. (2008). Splicing fidelity, enhancers, and disease. *Front. Biosci.* **13**, 1926-1942.
Thisse, C., Thisse, B., Halpern, M. E. and Postlethwait, J. H. (1994). Goosecoid expression in neurectoderm and mesendoderm is disrupted in zebrafish cyclops gastrulas. *Dev. Biol.* **164**, 420-429.
Tian, J., Yam, C., Balasundaram, G., Wang, H., Gore, A. and Sampath, K. (2003). A temperature-sensitive mutation in the nodal-related gene cyclops reveals that the floor plate is induced during gastrulation in zebrafish. *Development* **130**, 3331-3342.
van der Knaap, M. S., Pronk, J. C. and Scheper, G. C. (2006). Vanishing white matter disease. *Lancet Neurol.* **5**, 413-423.
Vogeli, K. M., Jin, S. W., Martin, G. R. and Stainier, D. Y. (2006). A common progenitor for haematopoietic and endothelial lineages in the zebrafish gastrula. *Nature* **443**, 337-339.
von Bubnoff, A. and Cho, K. W. (2001). Intracellular BMP signaling regulation in vertebrates: pathway or network? *Dev. Biol.* **239**, 1-14.
Watanabe, H., Shionyu, M., Kimura, T. and Kimata, K. (2007). Splicing factor 3b subunit 4 binds BMPR-IA and inhibits osteochondral cell differentiation. *J. Biol. Chem.* **282**, 20728-20738.
Weinberg, E. S., Allende, M. L., Kelly, C. S., Abdelhamid, A., Murakami, T., Andermann, P., Doerre, O. G., Grunwald, D. J. and Riggleman, B. (1996). Developmental regulation of zebrafish MyoD in wild-type, no tail and spadetail embryos. *Development* **122**, 271-280.
Winnier, G., Blessing, M., Labosky, P. A. and Hogan, B. L. (1995). Bone morphogenetic protein-4 is required for mesoderm formation and patterning in the mouse. *Genes Dev.* **9**, 2105-2116.